

ESTIMATION OF CRYOGENIC HEAT LOADS IN CRYOMODULE DUE TO THERMAL RADIATION *

A. Saini[†], V. Lebedev, N.Solyak, V. Yakovlev, Fermilab, IL 60510, USA

Abstract

Cryogenic system is one of major cost drivers in high intensity superconducting (SC) continuous wave (CW) accelerators. Thermal radiations coming through the warm-ends of cryomodule and room temperature parts of the power coupler result in additional cryogenic heat loads. Excessive heat load in 2K environment may degrade overall performance of the cavity. In this paper we present studies performed to estimate additional heat load at 2K due to thermal radiation in 650 MHz cavity cryomodule in high energy section of PIP-II SC linac.

INTRODUCTION

The Proton Improvement Plan -II (PIP-II) is proposed to develop a high intensity proton beam facility at Fermilab. It is primarily based on construction of 800 MeV CW SC linac that would initially operate in the pulse mode. A schematic of linac baseline configuration is shown in Fig. 1. It consists of room temperature front-end and SC linac. Each superconducting section in Fig. 1 is represented by optimal beta of respective cavities except for LB and HB sections where geometrical beta of corresponding cavities are shown. A detail description of baseline configuration of PIP-II SC linac is presented elsewhere [1].

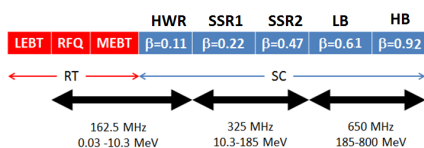


Figure 1: Technology map of PIP-II linac

All cryomodules in SC linac are connected by room temperature sections. This arrangement provides an option of possible beam collimation after each cryomodule which could help to minimize uncontrolled beam losses in cryogenic environment. Furthermore, it also provides space for additional beam diagnostics (transverse and longitudinal profile monitors, beam loss monitors, etc.).

GENERAL

The major infrastructure investment and the operational cost of a superconducting linear accelerator are outlined by its cryogenic requirements. As can be noticed from Table 1, the cryogenic efficiency is significantly lower at 2 K and it is required about 800 W of wall-plug power to remove every Watt of power dissipated in this environment. Consequently, cryogenic load at 2K derives size and therefore the cost of cryogenic-plant. While the dynamic cryogenic load at 2K

Table 1: Typical Cooling Efficiency at Different Cryogenic Temperatures

Temperature	2K	4K	70
Wall-plug power per Watt of power dissipation	800 W	250 W	25 W
Cryo- efficiency	0.125%	0.4%	4 %

is primarily determined by the RF power dissipation in an accelerating cavity, heat transfer due to conduction and radiation through various channels (Helium vessel supports, transfer lines, cables etc.) largely outlines the static heat load of cryomodule. Contribution of heat transfer through the convection is relatively negligible in cryomodule because of its vacuum vessel that maintain high vacuum for thermal insulation. A multilayer insulation using low emissivity material and intermediate temperature screenings (thermal shields) limit the radiation load in cryomodule. However, lateral radiation coming through the warm-ends of cryomodule and penetration of a room temperature surface into the cryogenic environment still result in an accountable radiation load. Heat transfer through the conduction can usually be estimated precisely, but estimation of the radiation heat load in a cryomodule is non-trivial and strongly affected by the geometry and the physical properties of a surface.

Insertions of warm section between cryomodules in PIP-II SC linac result in an increase of static cryogenic load due to lateral thermal radiation entering from both warm-ends of cryomodule. Room temperature parts of the power coupler also add radiation heat load. Radiation heat load in a cryomodule increases in proportion to cross-section area of beam pipe. Thus, radiation heat load for high beta (HB) 650 MHz cryomodules having beam pipe aperture of 118mm is higher than any other cryomodules in the SC linac. In this paper we present contribution of radiation to the cryogenic load at 2K in HB 650 MHz cryomodule and discuss its impact on overall performance of 5-cell elliptical shape HB 650 MHz cavity. This estimation allows us to take a decision on the requirement for 80 K thermal shield between HB cryomodules.

THERMAL RADIATION FROM CRYOMODULE WARM-ENDS

As shown in Fig. 2, niobium-beam pipe is not the part of helium jacket and it is cooled down by process of the conduction-cooling. Thus, heat removal in the niobium-beam pipe is not as efficient as in the cavity. Excessive heat deposition may rise temperature in the beam pipe that causes increase in the BCS surface resistance [2]. Consequently, RF

* Work supported by US DOE under contract DE- AC02-76CH03000.

[†] asaini@fnal.gov

power dissipation in the niobium-beam pipe is also increased that causes further rise in temperature. Thus, this process enters in a close loop and in a worst case, it leads to quenching of the niobium- beam pipe. A sudden rise in temperature of the beam pipe also enhances heat losses in the cavity due to conduction heating. Additional heat deposition in the cavity can degrade its quality factor (Q_0) and may ultimately result in a quench. In this section we estimate power deposition in the niobium-beam pipe of HB 650 MHz cavity due to thermal radiation coming from warm-ends of cryomodule and room temperature parts of the power coupler.

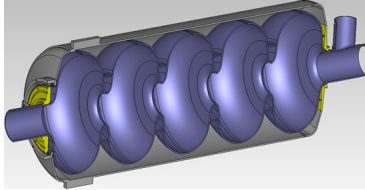


Figure 2: A superconducting cavity dressed with helium jacket.

The radiative heat transfer from one surface to another is expressed as following:

$$\dot{Q}_{1 \rightarrow 2} = \frac{\sigma \cdot (T_1^4 - T_2^4)}{\frac{(1-\epsilon_1)}{A_1 \epsilon_1} + \frac{(1-\epsilon_2)}{A_2 \epsilon_2} + \frac{1}{A_1 F_{1 \rightarrow 2}}}; \quad (1)$$

where $\dot{Q}_{1 \rightarrow 2}$ is radiative power on surface 2 from surface 1, T , ϵ , A are temperature, emissivity and area respectively for surface 1 and 2. $F_{1 \rightarrow 2}$ is view factor that determines proportion of radiation from surface 1 reaching to surface 2. If we assume there are no thermal shields between 2 K and 300K surfaces and both surfaces behave like the perfect black body, $\epsilon_1 = \epsilon_2 = 1$, maximum radiative power deposited to a niobium beam pipe is about 5W.

In order to make a more realistic estimation, study is performed using a simplified model of the cryomodule-end pipe in ANSYS [3]. As shown in Fig. 3, geometry of the cryomodule-end is segmented into several cylindrical pipes corresponding to respective thermal shields.

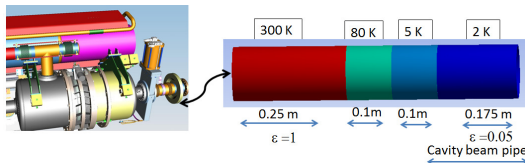


Figure 3: A simplified model of cryomodule-end in ANSYS.

The steady state surface to surface radiation boundary condition is applied. Thus, net radiation heat transfer (\dot{Q}_{net}) from a surface is given as:

$$\dot{Q}_{net} = \dot{Q}_{emitt} - \dot{Q}_{inc} + (1 - \epsilon)\dot{Q}_{inc}; \quad (2)$$

where \dot{Q}_{emitt} is rate of heat emitted and \dot{Q}_{inc} is rate of heat incident. Emissivity of niobium used in this analysis is 0.05 [4] and emissivity of the stainless steel beam pipes at 80 K and 5 K are varied in order to understand its impact on

radiation interception capability. Figure 4 shows radiative power deposition along niobium cavity beam pipe for three values of emissivity of stainless steel i.e. 1.0, 0.3 and 0.1. One can conclude from Fig. 4 that higher emissivity of stainless steel provides effective interception of radiation at 5K and 80K. Consequently, lower power is deposited to cavity beam pipe. A rough surface is better attenuator of radiation. Thus, chemical etching or sand blasting of stainless steel pipes may enhance their emissivity. However, a rough surface also increases conduction-heating but these losses are still tolerable at 80K and 5K environment.

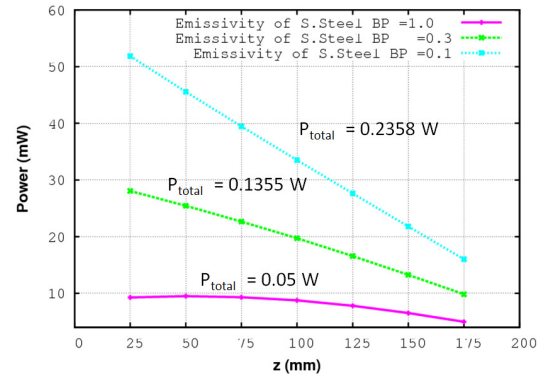


Figure 4: Radiative power deposition along niobium beam pipe for different emissivities of stainless steel pipe. P_{total} is total power deposited in beam pipe.

Temperature Profile in Niobium Beam Pipe

Temperature distribution in niobium beam pipe is evaluated using 1-D heat diffusion equation:

$$\frac{\partial}{\partial z} \left(K(T(z)) \frac{\partial T(z)}{\partial z} \right) dz = -(\dot{q}_{z+\delta z} - \dot{q}_z); \quad (3)$$

where \dot{q} is given as:

$$\dot{q} = \frac{1}{A} \epsilon P F_{12}(z); \quad (4)$$

P is radiative power reaching to niobium pipe, $F_{12}(z)$ is view factor from cylinder base to lateral surface, A is area and K is thermal conductivity of niobium. It can be observed

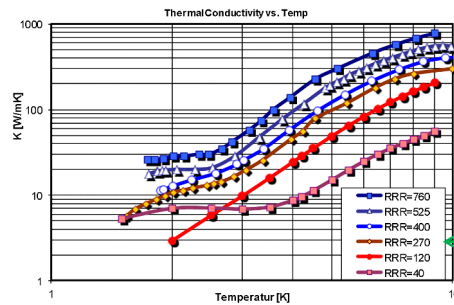


Figure 5: Variation in thermal conductivity with temperature for different RRR of niobium samples.

from Fig. 5 that thermal conductivity strongly depends on temperature. It also varies with residual resistance ratio (RRR) of material. Using the best fit to experimental data,

thermal conductivity of niobium corresponding to RRR of 270 is expressed as:

$$K(T) = \exp(C_1 + C_2(\log T) + C_3(\log T)^2 + C_4(\log T)^3 + C_5(\log T)^4 + C_6(\log T)^5); \quad (5)$$

where $C_1..C_6$ are fitting coefficients and their values are $-4.57848, 31.01, -54.77795, 46.41167, -17.89282$ and 2.56625 respectively.

Applying the boundary conditions: $T(z = 0) = 5K$; $T(z = L) = 2K$ and using equations 4 and 5, one can solve equation 3 numerically. For the radiation power of 2W (about 8 times higher than maximum estimated radiation power (Fig. 4).), temperature profile along niobium pipe is evaluated for different emissivity and shown in Fig. 6. We use wall thickness of 0.38 cm and length of 16 cm for the niobium pipe in this study. It can be observed from Fig. 7

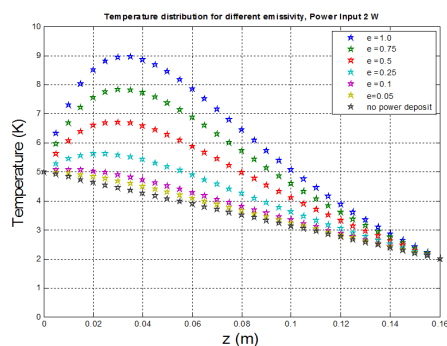


Figure 6: Temperature distributions along niobium beam pipe for different emissivity (ϵ).

that higher emissivity leads to an increase in maximum temperature of niobium pipe. The BCS surface resistance [2]

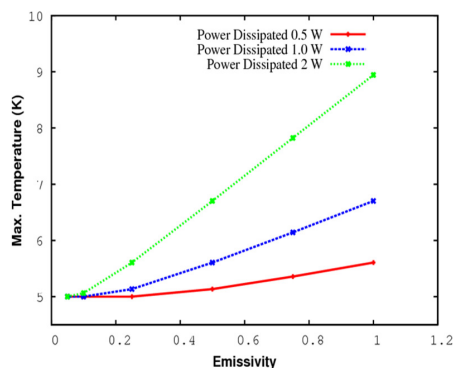


Figure 7: Variation in maximum temperature of niobium pipe with emissivity (ϵ) for different radiation power.

increases with rise in temperature. Figure 8 shows surface resistance along niobium pipe corresponding to temperature distributions shown in Fig. 6. RF fields of cavity decay in niobium pipe therefore, higher surface resistance implies higher RF power dissipation in niobium beam pipe. Figure 9 shows RF power dissipation along niobium pipe for fundamental mode (operating voltage of 17.5 MV in HB 650 MHz cavity.). Estimated quality factor in niobium pipe is about

three order higher than quality factor of cavity, $Q_0 = 2 \times 10^{10}$, at operating mode. Hence, cavity performance does not get affected from additional radiation load deposited in a niobium pipe.

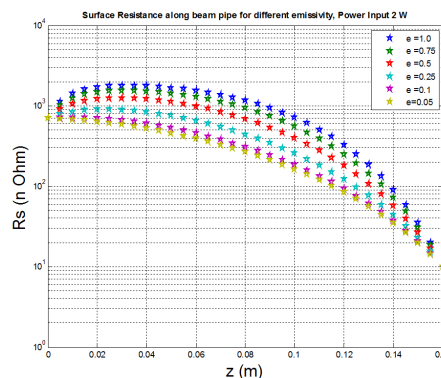


Figure 8: Variation in surface resistance along niobium pipe.

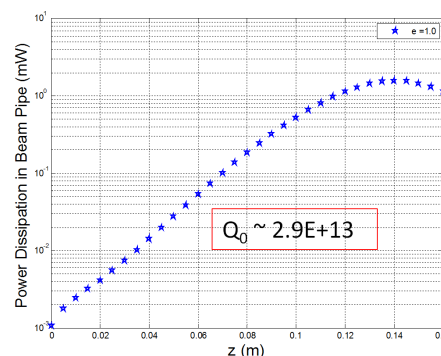


Figure 9: RF power dissipation along niobium beam pipe for the case when radiation power of 2 W is deposited and surface emissivity of niobium is considered to be one.

Thermal Radiation from Power Coupler

The power coupler for 650 MHz cavity consists of normal conducting parts such as ceramic window, antenna and antenna tip. A detailed description of the power coupler design is presented elsewhere [5]. A similar study is performed using ANSYS to quantify radiation load on niobium beam pipe due to normal conducting components of the power coupler. Using the emissivity of antenna and antenna tip equal to 0.1 and 1.0 for ceramic window, radiative power deposited to a niobium beam pipe is 0.15 W.

CONCLUSION

Evaluation of heat loads due to radiation coming through the warm-ends of cryomodule and normal conducting parts of the power coupler in the HB 650 cryomodule are performed using a simplified simulation model. The level of radiation power deposited to the niobium cavity beam pipe is moderate. Even, power deposition of 2 W in niobium pipe does not result in significant enhancement of RF losses. In conclusion, there is no need for additional 80 K thermal shield to cover the warm-section between the HB cryomodules.

REFERENCES

- [1] S.D. Holmes, V. Lebedev et al., "Proton Improvement Plan -II Reference Design Report", *Project-X-doc-1370*.
- [2] H. Padamsee, J. Knobloch, T. Hays, *RF Superconductivity for Accelerators*, (WILEY-VCH, 2008).
- [3] <http://www.ansys.com/>
- [4] M.-H. Chang, C. Wang et al, IEEE Transaction on Applied Superconductivity, vol. 21, no. 3, page no. 1908 (2011).
- [5] S. Kazakov et al., "High Power Couplers for Project X", TUPO006, SRF'11, Chicago, USA (2011).